Changes in Schwann Cells and Vessels in Lead Neuropathy

HENRY C. POWELL, MB, BCh,
ROBERT R. MYERS, PhD,
and PETER W. LAMPERT, PhD

Departments of Pathology, Neurosciences, and Anesthesiology, University of California, San Diego, Veterans Administration Medical Center, La Jolla, California

Transmission electron microscopy (TEM) of peripheral nerve in rats receiving 6% lead carbonate for 4–10 weeks provided evidence of a specific Schwann cell injury, associated with demyelination. Intranuclear inclusions in Schwann cells appeared within 2 weeks of administration of a lead-containing diet. Swelling of Schwann cells and disintegration of their cytoplasm was evident at 4 weeks. Distinctive electron-dense inclusions appeared in both Schwann and endothelial cells during the period of intoxication and were ultrastructurally identical to pathognomonic inclusions of lead poisoning seen in renal tubular epithelial cells. Scanning microscopy (SEM) with electron-probe microanalysis was used to identify the lead-containing deposits. In addition to Schwann cell changes, vessels revealed endothelial cell injury and altered permeability to macromolecules. Since morphologic changes of Schwann cells precede the development of altered vascular permeability and endoneurial edema, it appears that lead gains access to the endoneurium prior to the development of altered vascular permeability, suggesting that edema and altered endoneurial fluid pressure are epiphenomena that supervene after demyelination occurs. Remyelination, Schwann cell proliferation and formation of onion bulbs are manifestations of persistent toxic injury to myelin-sustaining cells, resulting in chronic demyelination. (Am J Pathol 1982, 109:193–205)

EXPERIMENTAL LEAD NEUROPATHY is the prototype for toxic disorders in which demyelination occurs associated with injury to Schwann cells. Both degenerative and proliferative changes of Schwann cells have been described concomitant with demyelination and remyelination.[1] The former have been shown by electron microscopy to comprise swelling of Schwann cell cytoplasm and disruption of compact myelin, with loosening of individual myelin lamellae. Recently a specific change in Schwann cells was noted: distinctive intranuclear inclusions composed of electron-dense material consistent with lead-protein complexes.[2] These bodies resemble intranuclear deposits discovered in liver and kidney tissues of children afflicted with lead poisoning.[3] Their significance has received special attention in lead nephropathy,[4] in which evidence for a protective role by intranuclear lead–nucleoprotein complexes had been adduced. Unlike free lead, which may damage organelles and enzyme systems, protein-bound lead in intranuclear inclusions is believed to be inactive.[5,6]

The present experiments were designed to compare renal and Schwann cell intranuclear inclusions in the same animals and to identify lead deposits by electron probe microanalysis. The role of such inclusions in Schwann cells is of particular interest, since they suggest a primary Schwann cell injury. Finally, the temporal sequence of intranuclear inclusions, Schwann cell swelling, and demyelination was analyzed and revealed that lead intoxication of Schwann cells precedes breakdown of the myelin sheath.

Materials and Methods

Forty adult, Long-Evans rats received a powdered laboratory diet containing 6% lead carbonate. Age-matched controls received the same powdered diet

Supported by grants NS 14162, NS 09053, and NS 07078 from the NINCDS and the Veterans Administration Research Service and aided by a Basil O'Conner Starter Research grant from the National Foundation–March of Dimes.

Accepted for publication June 17, 1982.

Address reprint requests to Henry C. Powell, MB, BCh, Department of Pathology, M-012, School of Medicine, University of California, San Diego, La Jolla, CA 92093.

0002-9440/82/1110-0193

without lead supplements. The left sciatic nerve and a section of kidney were removed from rats under deep anesthesia and fixed in freshly prepared 2.5% phosphate-buffered glutaraldehyde. Specimens were taken at weekly intervals from 1 to 11 weeks from separate rats sacrificed at those time points.

Preparation of Specimens for X-ray Microanalysis

We removed the right sciatic nerve separately and "quick-froze" it by mounting it on a cryostat chuck and inserting it into isopentane chilled by liquid nitrogen. Later, frozen sections were cut and placed on carbon stubs for insertion into an ETEC scanning electron microscope equipped with a Kevex detector for electron probe microanalysis. The detector area was 30 sq mm, and the detector window was 0.008 mm. The collection period was 60 seconds, and the electron microscope's accelerating voltage was 20 kev. We dehydrated unstained frozen sections by inserting them directly into the scanning electron microscope column. We then scanned the sections to identify areas of increased electron density corresponding to intranuclear inclusions. Electron probe

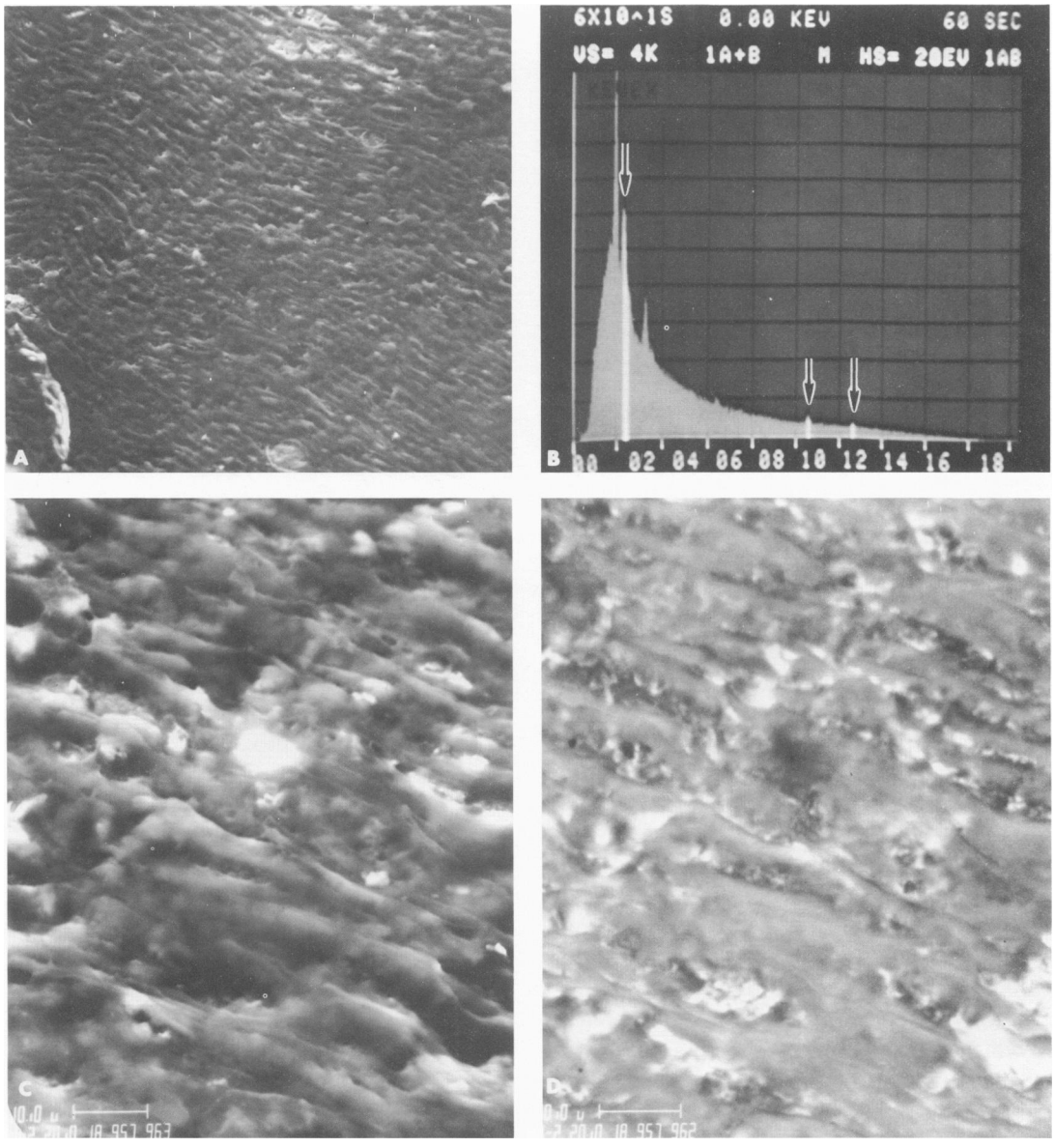

Figure 1A — Cryostat section of unstained quick-frozen sciatic nerve from a Long-Evans rat fed 6% lead carbonate for 7 weeks. Note the characteristic "wavy" pattern of peripheral nerve. **B** — Electron probe microanalysis of densities illustrated in **C** and **D** reveal three peaks (*arrows*) representing the M and L peaks; characteristic peaks for phosphorus, calcium, and iron can also be observed. **C** — Higher magnification of peripheral nerve section shown in **A** reveals nerve fibers in longitudinal array. A focal density on the long axis of a nerve fiber can be seen at the center. **D** — Backscatter imaging of the field illustrated in **C** showing the focal density analyzed in **B**.

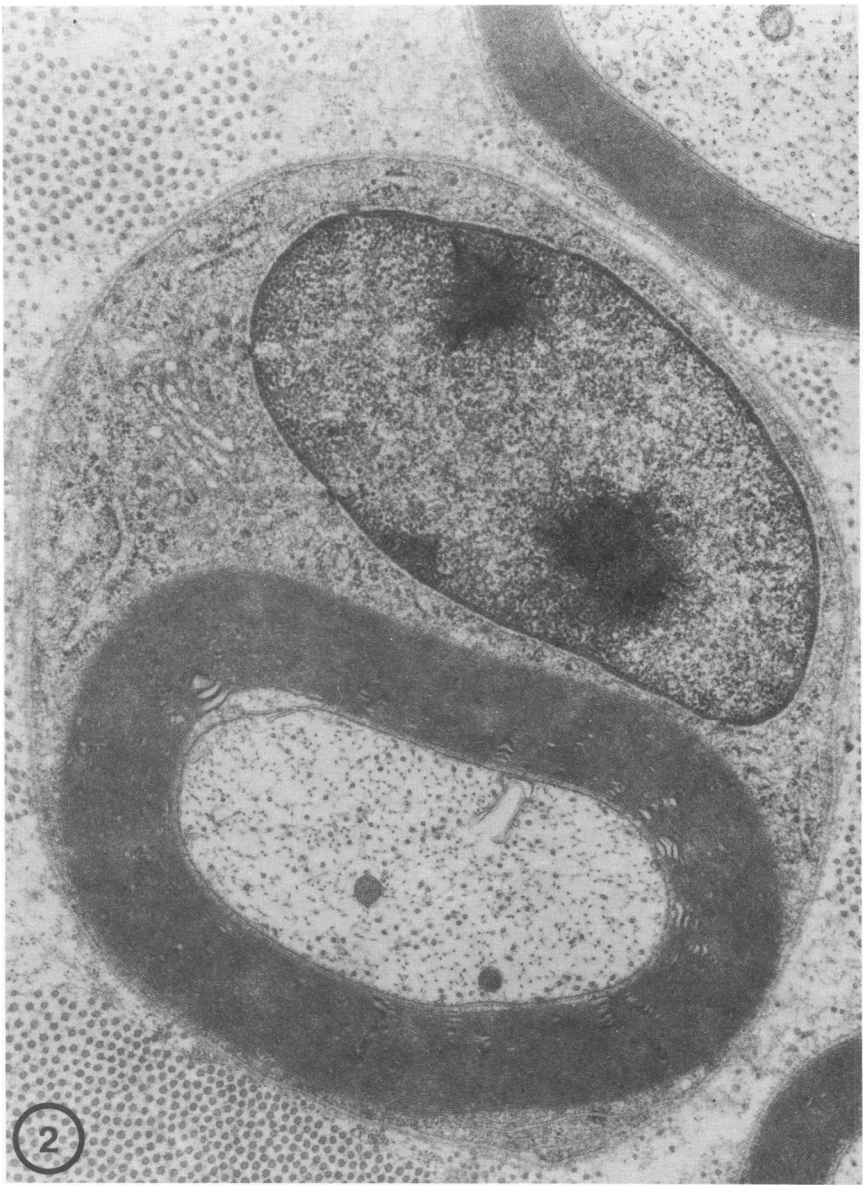

Figure 2—Two spicular, electron-dense inclusions are visible in a Schwann cell surrounding a normally myelinated axon. Rat sciatic nerve 9 weeks after initiation of a diet of 6% $PbCO_3$. (Uranyl acetate and lead citrate, ×21,000)

microanalysis then was used to resolve the elemental constituents of these deposits.

Electron Microscopy

Tissue from the left sciatic nerve was fixed in 2.5% glutaraldehyde for several hours then rinsed overnight in phosphate buffer at 4 C. The next day the tissue was postfixed in osmium tetroxide and dehydrated in serial concentrations of alcohol and propylene oxide prior to infiltration with and embedding in araldite resin for electron microscopy.

Permeability Studies

To investigate altered vascular permeability, we suspended 75 mg of horseradish peroxidase (HRP) in 1 ml normal saline and injected it into the jugular vein of selected experimental rats and controls. The tracer was allowed to circulate for 1 hour prior to excision of the nerve. The tissue was placed in 1.5% 0.1 M phosphate-buffered glutaraldehyde for 4 hours and then transferred to 5% phosphate buffered sucrose for 12 hours before being sectioned into 15–30-μ slices for further processing. Hanker–Yates reagent (Polysciences) was used to form the HRP enzyme–substrate complex. Otherwise, nerve sections were processed as described above for electron microscopic examination. One-micron-thick sections of araldite-embedded material were examined from each of the animals used in this study. Sections of kidney were stained with toluidine blue, and sections of nerve were stained with paraphenylene diamine.

Ultrathin sections for electron microscopy were stained with uranyl citrate and in some instances lead citrate, but the latter stain was withheld from some samples in which morphologic characteristics of the intranuclear inclusions were being examined.

Results

Electron Probe Microanalysis

Unstained cryostat sections of quick-frozen nerve were examined in a scanning electron microscope. The characteristic wavy outline of peripheral nerve was readily discernible at low magnification (Figure 1A). At higher magnification individual fibers were recognizable, and focal electron-dense deposits were apparent. These could be visualized both in the standard views and in the backscatter mode. Electron probe microanalysis of these densities yielded characteristic X-ray spectra for lead (Figure 1B). Peaks for calcium and phosphorus were also identified in electron-dense inclusions. Three characteristic peaks were visualized: the M line at 2.5 and two L lines at 10.6 and 12.8.

Electron Microscopy

Ultrathin sections of sciatic nerve were examined from animals sacrificed at 1–4, 7, 9, 10, and 11 weeks. Transmission electron microscopic examina-

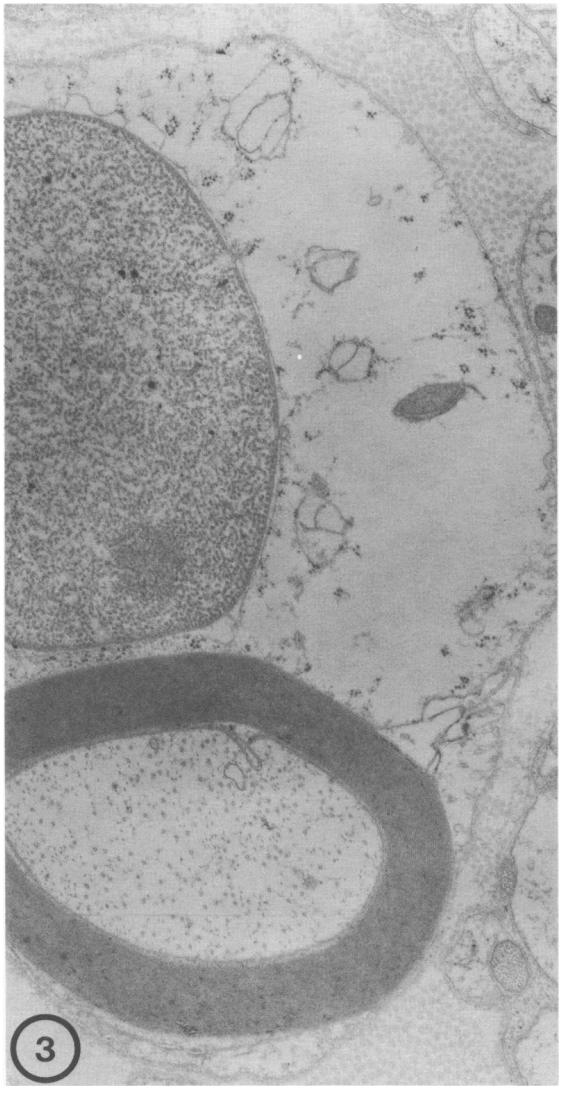

Figure 3—Swollen electron-lucent cytoplasm, characteristic of edema, affects this Schwann cell; however, the axon and myelin sheath appear unaffected. Rat sciatic nerve 4 weeks after commencement of a diet of 6% lead carbonate (Uranyl acetate and lead citrate, ×12,000) **Figure 4**—Loosening of myelin lamellae and development of intramyelinic vacuoles. The adjacent Schwann cell cytoplasm contains electron-dense bodies and vacuoles. Note the normal-appearing axon. Rat sciatic nerve after 10 weeks of poisoning with 6% $PbCO_3$. (Uranyl acetate and lead citrate, ×10,000) (Both with a photographic reduction of 3%)

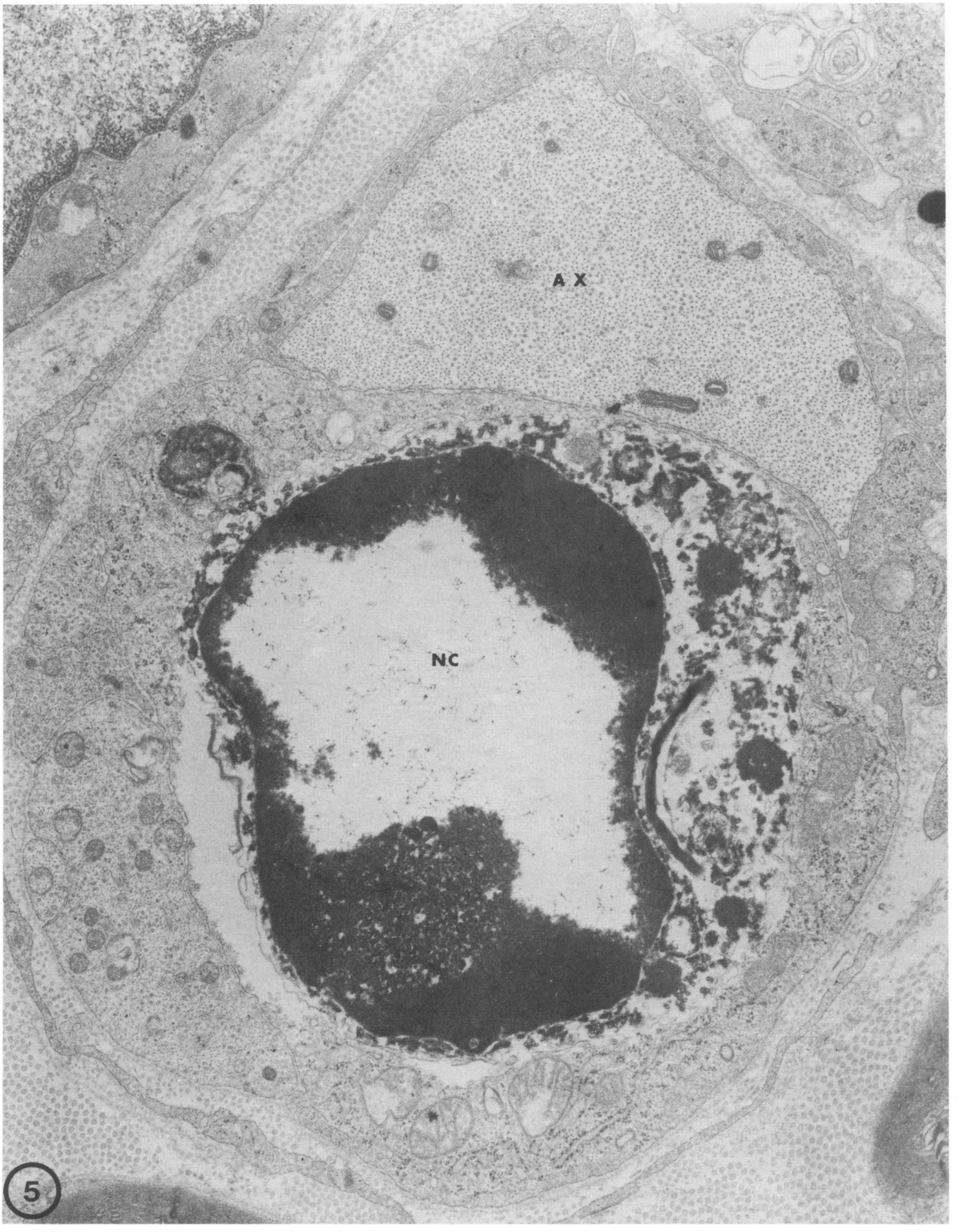

Figure 5—A necrotic cell (*NC*) is present within the neurilemmal tube, which also contains a normal-appearing axon (*AX*) and portions of other cells whose identity is uncertain. (Uranyl acetate and lead citrate, ×24,000)

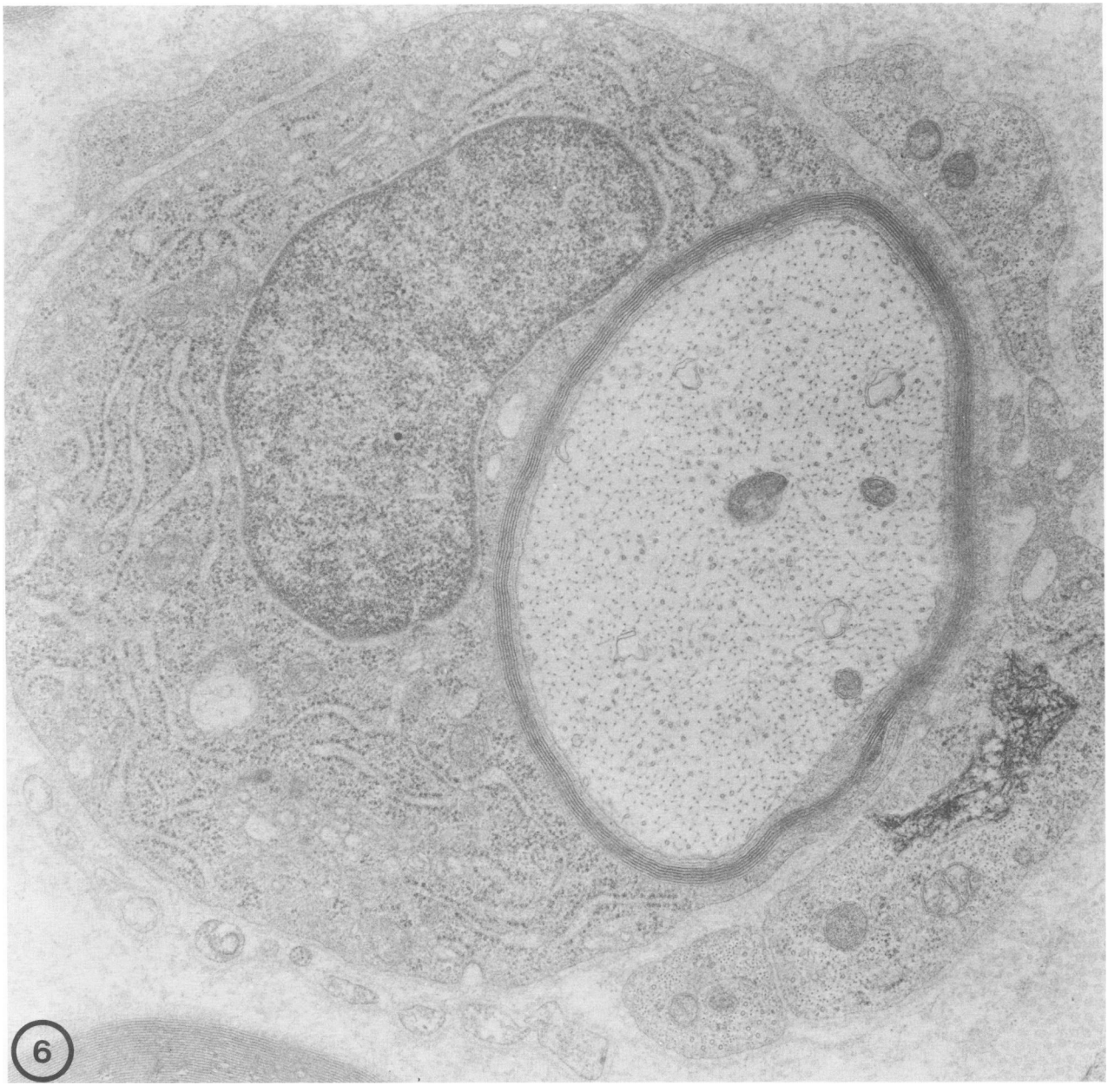

Figure 6—Onion bulb containing a remyelinating axon, defined by its thin myelin sheath. The Schwann cell shows reactive changes; there is increased cytoplasmic volume with prominent cisterns of endoplasmic reticulum. One of the surrounding Schwann cells contains a cytoplasmic electron-dense inclusion characteristic of lead intoxication. Rat sciatic nerve, 11 weeks after intoxication. (Uranyl acetate and lead citrate, ×27,500) (With a photographic reduction of 4%)

tion of aldehyde-fixed nerves revealed changes in Schwann cells, endothelial cells, and pericytes of the vasa nervorum. The earliest changes in Schwann cells were detected at 1 week. They included increased cytoplasmic volume with prominent endoplasmic reticulum, increased amounts of Golgi apparatus, fat droplets, large smooth-surfaced nuclei with prominent nucleoli, but no inclusions. These changes were interpreted as reactive. Intranuclear inclusions in Schwann cells were observed first at 2 weeks of intoxication and appeared in nerves at all the later time points in this study. Large electron-dense intranuclear inclusions were conspicuous both in normal-appearing (Figure 2) and morphologically abnormal Schwann cells. The inclusions consisted of a densely interwoven mass of irregularly shaped fibrils, some of which radiated out into the adjacent nucleoplasm. They could be distinguished from nucleoli, which were less electron-dense and lacked the spicular profile. Omission of lead citrate from staining accen-

Figure 7—Signs of lead intoxication in this capillary include an electron-dense inclusion (*arrow*) in the nucleus (*N*) of an endothelial cell and electron-dense bodies consistent with basophilic stippling in an erythrocyte (*E*). There is some thickening of endothelial cells and pericytes (*P*). Rat sciatic nerve, 9 weeks after lead intoxication. (Uranyl acetate and lead citrate, × 15,000)

tuated the contrast between the inclusions and chromatin. Both reactive changes and cytoplasmic swelling could be found at 3 weeks. More pathologic changes of Schwann cells were noted as early as 4 weeks after commencing the lead diet. They included cytoplasmic swelling and disintegration of organelles (Figure 3), leaving large electron-lucent areas of cytoplasm consistent with edema. Although Schwann cell changes were apparent in the early weeks of lead poisoning, breakdown of myelin sheaths was uncommon before 9 weeks. After 9 weeks, disintegration of myelin, with development of interlamellar electron-lucent spaces occurred, associated with cytoplasmic abnormalities (Figure 4). Necrotic cells within the

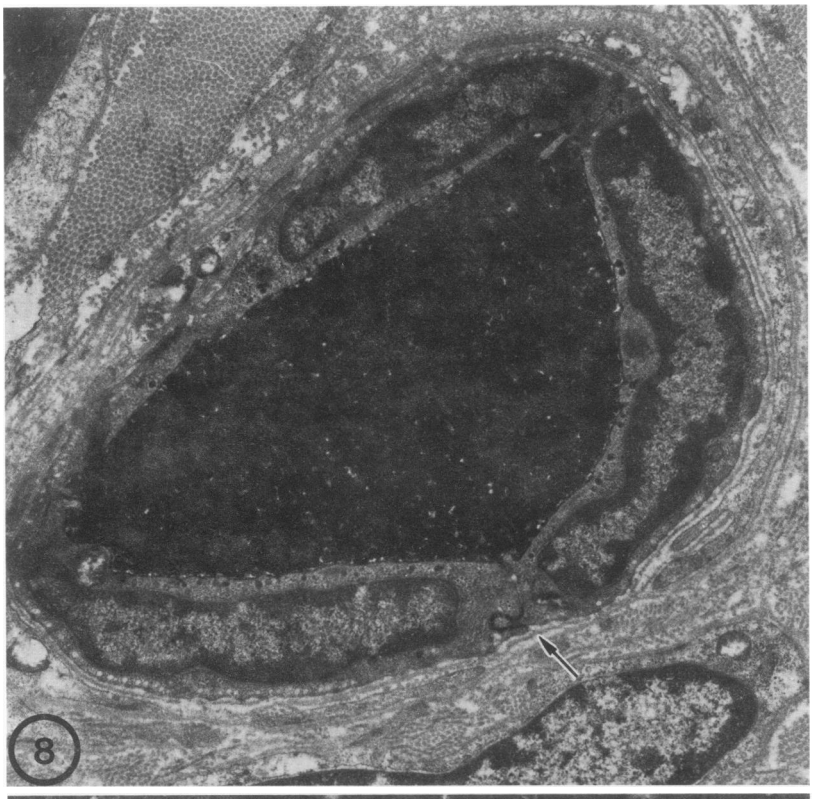

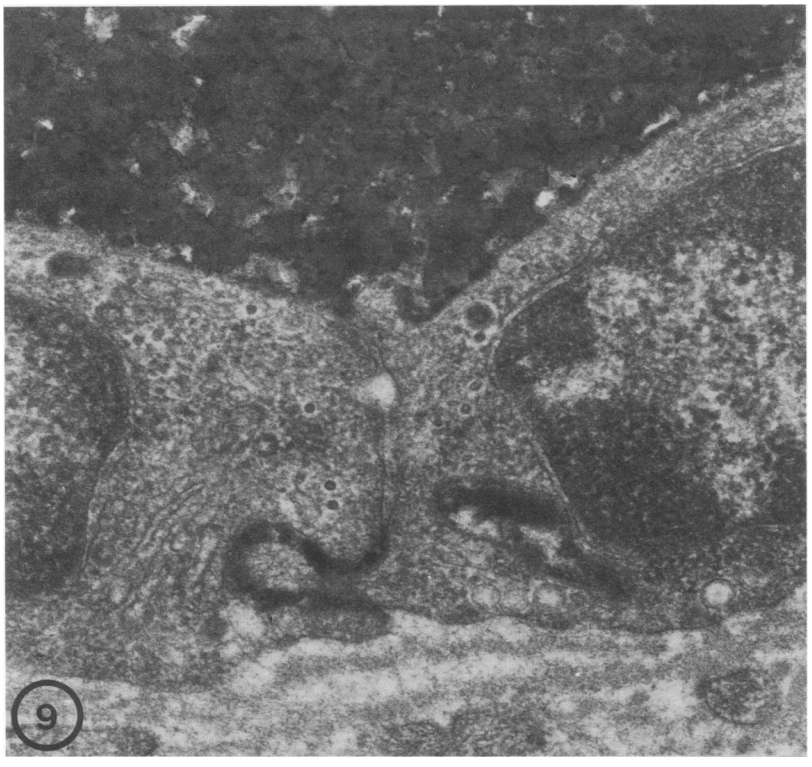

Figure 8—Endoneurial capillary from a rat sciatic nerve after injection of HRP prior to sacrifice. The lumen is filled with HRP reaction product, and interendothelial cell leakage can be seen (*arrow*). Rat sciatic nerve, 11 weeks after intoxication. (Uranyl acetate and lead citrate, ×14,000) **Figure 9**—Higher power electron micrograph depicting interendothelial cell leakage shown in Figure 8. (×90,000)

neurilemmal tube were also observed (Figure 5). Intracytoplasmic fibrillar electron-dense inclusions were present in Schwann cells also (Figure 6). These inclusions were less frequent than intranuclear inclusions and were sometimes observed in redundant Schwann cells of an onion bulb (Figure 6). Demyelination and remyelination were commonly seen in material sampled from 7–11 weeks (Figure 5 and 6).

Microangiopathic changes were pronounced in nerves excised during this period. Morphologic

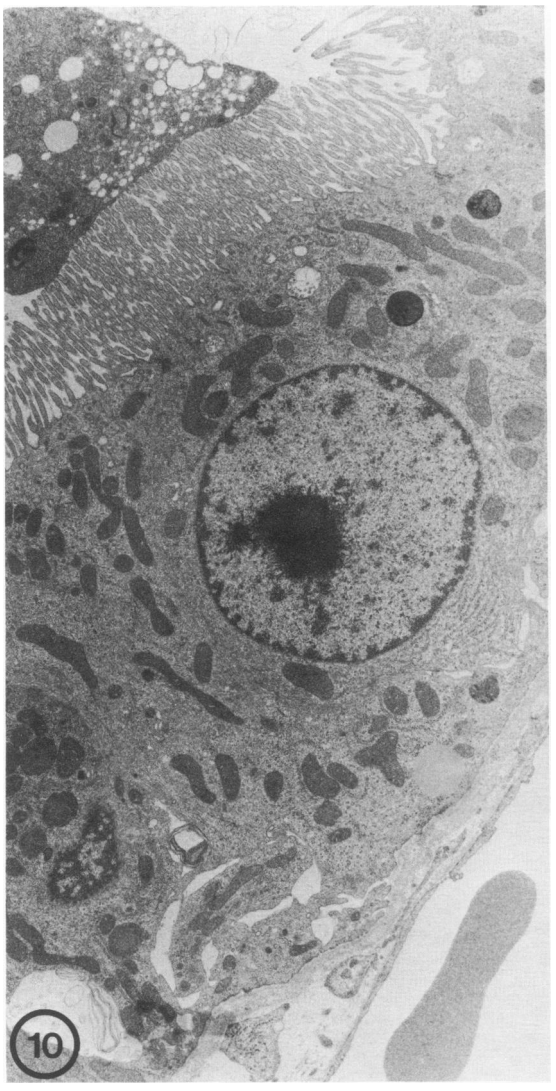

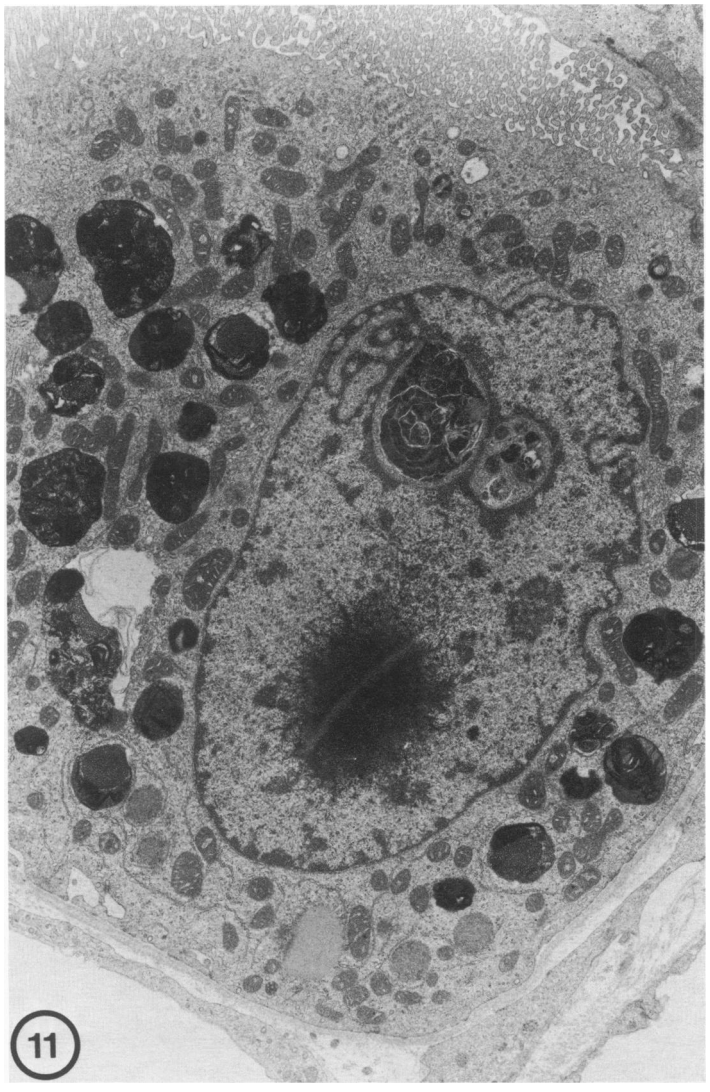

Figure 10 – Renal tubular cell from a rat kidney after 11 weeks of 6% lead carbonate. An intranuclear inclusion and many intracytoplasmic dense bodies are visible. (Uranyl acetate and lead citrate, ×8000) **Figure 11** – Renal tubular epithelial cell with intranuclear inclusions characteristic of lead poisoning. A necrotic cell rests on the brush border. Occasional dense bodies and a lipid droplet appear in the cytoplasm. Rat kidney, after 9 weeks of lead intoxication. (Uranyl acetate and lead citrate, ×7000) (With a photographic reduction of 3%)

changes were observed in endothelial cells, pericytes, and erythrocytes, which showed focal electron-dense deposits consistent with basophilic stippling. Endothelial cells contained both intranuclear inclusions (Figure 7) and intracytoplasmic fibrillar inclusions. Intranuclear inclusions in endothelia were first detectable after 1 week. Progressive thickening of vessel walls was visible by light-microscopic examination in ensuing weeks. The cytoplasm of both endothelial cells and pericytes contained numerous intermediate cytoplasmic filaments and pinocytotic vesicles. Inclusions were not observed in pericyte nuclei or cytoplasm. Leakage of horseradish peroxidase between endothelial cells was also demonstrated (Figures 8 and 9) at this time (9–11 weeks). No interendothelial cell leakage was observed in controls injected with HRP. Supernumerary layers of basement membrane (Figure 9) contributed to the increased thickness of vessel walls. Proximal renal tubular epithelium was also examined for the presence of intranuclear inclusions. Numerous darkly staining inclusions were visible by light microscopic examination in renal tubular epithelium and were readily detectable upon electron-microscopic examination. The inclusions appeared identical to those observed in Schwann and endothelial cells, with strongly electron-dense cores and filamentous surfaces radiating into the surrounding nucleoplasm (Figures 10 and 11). Smooth-surfaced, electron-dense bodies resembling autophagic vacuoles were also numerous in renal cell cytoplasm

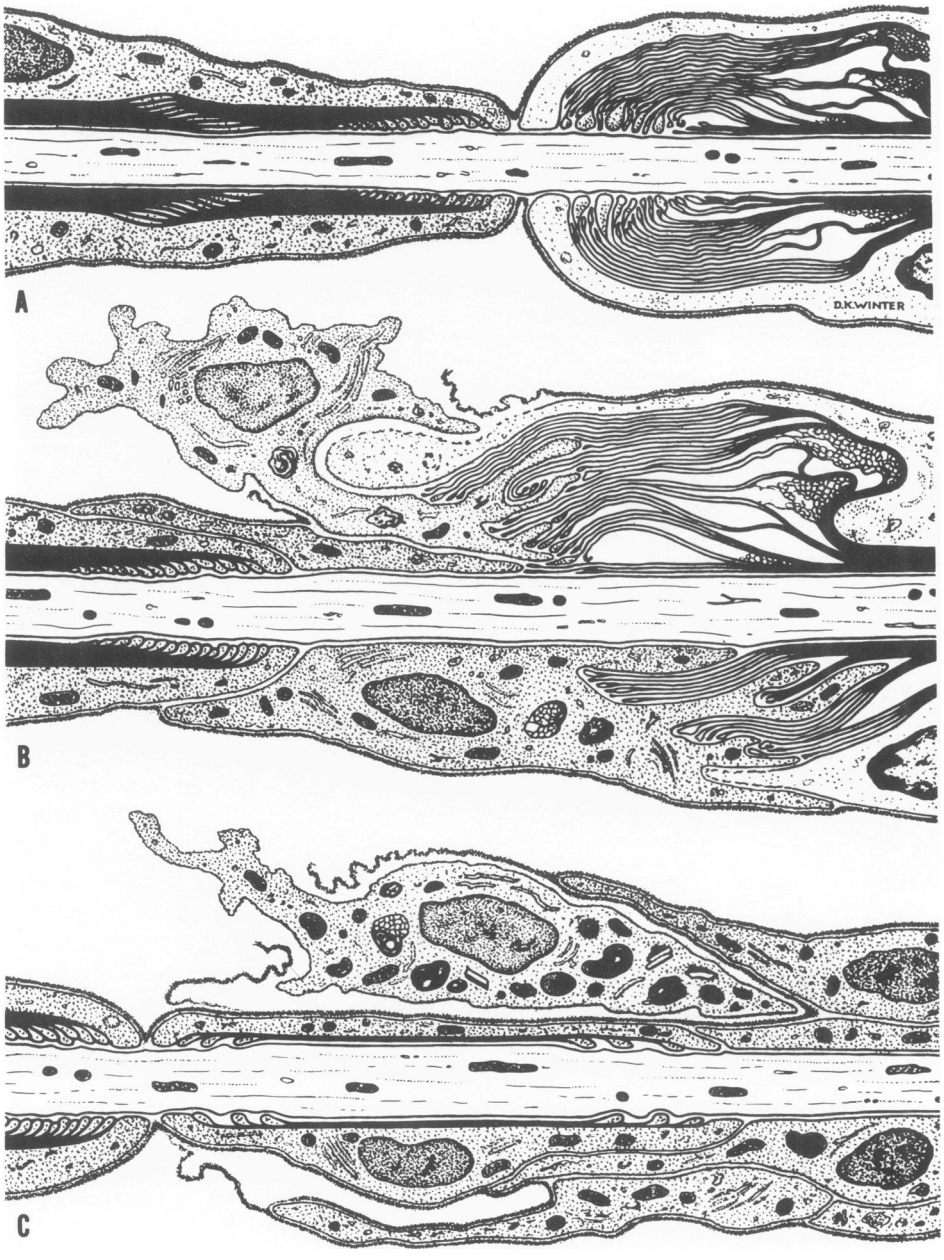

Figure 12A—Disintegration of the myelin segment (*to the right*) associated with swelling of Schwann cell cytoplasm in early lead intoxication. **B**—Penetration of the neurilemmal tube by macrophages, with stripping of disintegrating myelin sheath. **C**—Proliferation of Schwann cells growing along persistent basement membranes and around the denuded axon, forming a new myelin sheath.

(Figure 10). Disintegration of myelin, Schwann cell proliferation, and formation of onion bulbs were observed after 10 weeks of intoxication. The cytoplasmic processes of supernumerary Schwann cells enveloped both normal and remyelinating as well as demyelinated axons (Figures 5 and 6). Cytoplasmic extensions, often arising from more than one proliferated Schwann cell were found within the basal lamina of the original neurilemmal tube. Some Schwann cells were rich in ribosomes, granular endoplasmic reticulum, and mitochondria (Figure 6). These changes may be reactive phenomena, but evidence of cytoplasmic injury was also present with electron-dense intracytoplasmic filaments (Figure 6), which are comparable to the intranuclear electron-dense deposits.

Discussion

Electron-microscopic study of peripheral nerve during the first 3 months of lead intoxication provided further evidence that specific injury to the

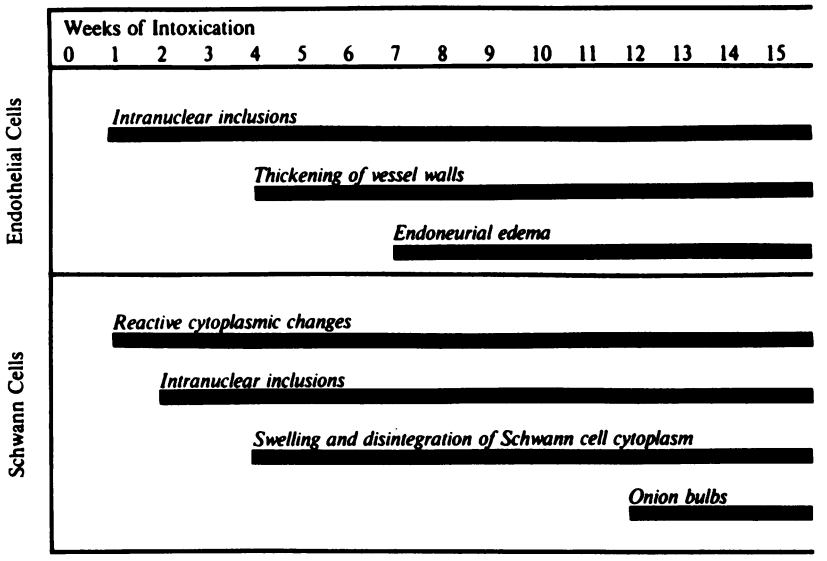

Figure 13—Sequence of pathologic change observed by electron microscopy in rat peripheral nerve during the first 15 weeks of lead intoxication.

myelin-sustaining Schwann cells is the primary pathologic event in this neuropathy. Schwann cell swelling and cytoplasmic disintegration (Figures 3 and 4) and intranuclear inclusions are detectable before altered vascular permeability and elevated endoneurial fluid pressure supervene. Lead-rich intranuclear inclusions represent the most specific indication of primary Schwann cell injury. That such injuries to Schwann cells are detected at 2 weeks, whereas altered vascular permeability and edema were not found until 7 weeks, suggests that lead gains access to the endoneurium early in the neuropathy and that increased permeability of the blood–nerve barrier and edema are epiphenomena. As reported by Windebank and associates,[7] the highest concentrations of lead were found in nerve during the early weeks of intoxication.[7] Although the mechanism is not known, lead appears to traverse the blood–nerve barrier and acumulate in the endoneurium before altered permeability can be demonstrated at 7 weeks.[2] In the following paragraphs we will discuss 1) the comparative ultrastructure of lead-bearing intranuclear inclusions in Schwann cells, renal epithelium, and vascular endothelium; 2) the microangiopathy of lead neuropathy; and 3) the mechanism of demyelination in this toxic Schwannopathy.

Eosinophilic intranuclear inclusions were first recognized about fifty years ago during microscopic examination of autopsied liver and kidney from children who died of lead poisoning.[3] By combining morphologic, biochemical, and other techniques, various investigators have shown these inclusions to contain high concentrations of lead, bound to certain proteins.[5] Both autoradiography[8] and electron probe microanalysis[9] have been used to detect lead in renal tubular intranuclear inclusions. Early reports of this phenomenon described these inclusions as acid-fast, and subsequent analysis revealed them to contain protein other than nucleoprotein. The lead concentration of renal inclusions was reported to be about 50 μg lead/mg protein.[6] Formation of these inclusions has been suggested to serve as a protective mechanism during the transcellular transport of lead.[5,6] According to this hypothesis, free lead incorporated into a lead–protein complex is no longer diffusible, and this mechanism of concentration of lead is thought to protect mitochondrial respiration and protein synthesis. In fact, when low concentrations of lead were fed to rats, lead-bearing intranuclear inclusions in kidneys appeared before other recognized abnormalities such as decelerated weight gain, increased amino-laevulinic acid excretion, reticulosis, and renal edema.[5,6] It is therefore of interest that in this neuropathy intranuclear inclusions appeared first in cells showing no other morphologic abnormalities (Figure 2). Our observation that they were most numerous during the early weeks of lead intoxication is consistent with previously published reports of intraneural lead accumulation.[7] Windebank and his colleagues analyzed endoneurial lead content in rats receiving 4% lead carbonate and found significantly increased lead as early as 5 days after dietary intoxication commenced. Lead levels were maximum at 35 days.[7] At that point, the endoneurial lead concentration was almost 10 times greater than blood lead levels. They suggested that

"lead molecules are bound or trapped within the endoneurium." The presence of both endothelial and Schwann cell intranuclear inclusions as early as 1–2 weeks after intoxication is consistent with their hypothesis. We found inclusions in endothelial cells at 1 week and the earliest Schwann cell inclusions 2 weeks after intoxication. Reactive changes in Schwann cells were observable at 1 week; however, degenerative changes in Schwann cell cytoplasm were not apparent until 3–4 weeks after intoxication. It appears that inclusions are most conspicuous during the early months of lead intoxication and that their occurrence predates Schwann cell damage and disintegration of myelin sheaths.

Intracytoplasmic inclusions composed of electron-dense fibrils were also observed in Schwann cell cytoplasm (Figure 6) and in renal and endothelial cells. Identical deposits have been shown previously in renal cells,[11] in which they appear as early as 6–8 hours after intracardiac injection into rats and mice.[12] The presence of intranuclear and intracytoplasmic inclusions in the early stages of lead neuropathy is of interest because of the microangiopathy that subsequently develops, in which altered permeability and progressive thickening of vessel walls are the principal abnormalities. The cellular changes of the vasa nervorum, involving intoxication and proliferation, may be compared to "onion bulb" changes.

One of the hallmarks of lead neuropathy is the "onion bulb" dysplasia of Schwann cells associated with chronic lead administration. The pathogenesis of onion bulb formation is related to repetitive toxic injury.[1,13] After destruction of the Schwann cell, its basal lamina persists around demyelinated axons. Proliferating Schwann cells originating from dividing cells of adjacent internodal segments wrap around denuded axons to form new myelin sheaths. Other Schwann cells growing along the persistent basal lamina create an outer ring of Schwann cell processes. Repeated injury by lead poisoning may affect either the innermost Schwann cell that remyelinated the central axon or the Schwann cell that grew along the preexisting basal lamina. Yet another persistent basal lamina remains after disintegration of the second generation of Schwann cells and provides an additional scaffolding for the next wave of proliferating cells (Figure 12).

Electron-microscopic examination (Figure 13) also disclosed morphologic abnormality of endothelial cells and pericytes in the vasa nervorum. Changes in these cells included interendothelial cell leakage of plasma-borne horseradish peroxidase, proliferation of endothelium, and pericytes with accumulation of filaments and other structures in their cytoplasm. Filamentous dysplasia was even more striking in the pericytes, and both types of cells showed reduplication of their basal lamina.

Endoneurial edema appears to be the result of endothelial cell injury and first appears after about 50 days.[2,7,10] However, the neuropathy is already established, with evidence of Schwann cell injury, segmental demyelination, and onion bulb formation prior to development of altered permeability.

X-ray microanalysis has been used previously to detect lead deposits in rat brain and cerebral capillaries.[14,15] However, this work was performed with tissue already fixed for electron microscopy and included contaminants. In addition to lead, osmium and other elements were found. Since the peaks for osmium lie very close to lead in the spectrum, we chose to avoid possible contamination by using frozen sections mounted on carbon stubs. The results show calcium and phosphorus deposition as well as lead. These elements have been reported in lead deposits in previous X-ray microanalytic observations,[14,15] and their presence may have pathologic significance.

Segmental demyelination can be divided into conditions in which the myelin itself is the primary target of a toxin or immune process[13] and those in which Schwann cells are the principal target, such as lead neuropathy. Although endothelial cells and pericytes are damaged, the most notable injury is to Schwann cells. As a result, myelin sheaths degenerate, and their disintegration is accompanied by the entry of macrophages into the neurilemmal tube (Figures 5 and 12). These cells remove damaged myelin and necrotic Schwann cell debris. The ultrastructural findings reported here are consistent with initial Schwann cell injury (Figure 3) followed by subsequent disintegration of myelin. Lead-bearing inclusions in Schwann and endothelial cells are the most specific findings in the cytopathogenesis of this neuropathy, in which demyelination, endoneurial edema, and microangiopathy are the principal abnormalities.

References

1. Lampert PW, Schochet SS: Demyelination and remyelination in lead neuropathy. J Neuropathol Exp Neurol 1968, 27:527–545
2. Myers RR, Powell HC, Shapiro HM, Costello ML, Lampert PW: Changes in endoneurial fluid pressure, permeability and peripheral nerve ultrastructure in experimental lead neuropathy. Ann Neurol 1980, 8:392–401

3. Blackman SS Jr: Intranuclear inclusion bodies and the kidney and liver caused by lead poisoning. Bull Johns Hopkins Hosp 1936, 38:384–406
4. Goyer RA, May P, Cates MM, Krigman MR: Lead and protein content of isolated intranuclear inclusion bodies from kidneys of lead poisoned rats. Lab Invest 1970, 22:245–251
5. Goyer RA, Moore JF, Barrow EM: Lead binding protein in the lead induced intranuclear inclusion body. Am J Pathol 1971, 62:96a–97a
6. Goyer RA, Leonard DL, Moore JF, Rhyne B, Krigman MR: Lead dosage and the role of the intranuclear inclusion body. Arch Environ Health 1970, 20:705–711
7. Windebank A, McCall JT, Hunder HE, Dyck PJ: The endoneurial content of lead related to the onset and severity of demyelination. J Neuropathol Exp Neurol 1980, 39:692–699
8. Dallenbach FD: Uptake of radioactive lead by tubular epithelium of the kidney. Am J Pathol 1974, 74:215–233
9. Carroll KG, Spwielli FR, Goyer RA: Electron probe microanalyzer location of lead in kidney tissue of poisoned rats. Nature 1970, 227:1056
10. Low PA, Dyck PJ: Increased endoneurial fluid pressure in experimental lead neuropathy. Nature 1977, 269:427–428
11. Richter GW: Evolution of cytoplasmic bodies induced by lead in rat and mouse kidneys. Am J Pathol 1976, 83:135–148
12. Choie DD, Richter GW: Lead poisoning: Rapid formation of intranuclear inclusions. Science 1972, 177:1194–1195
13. Lampert PW, Braheny SL, Powell HC: Neuropathies caused by myelinotoxic agents, Current Topics in Nerve and Muscle Research. Edited by AH Aguayo, K Karpati. Amsterdam, Excerpta Medica, International Congress Series, 1979, 455:292–298
14. Silbergeld EK, Wolinsky JS, Goldstein GW: Electron probe microanalysis of isolated capillaries poisoned with lead. Brain Res 1980, 189:369–376
15. Holtzman D, Herman MM, Hsu JS, Mortell P: The pathogenesis of lead encephalopathy: Effects of lead carbonate feeding on morphology, lead content, and mitochondrial respiration in brains of immature and adult rats. Virchows Arch (Pathol Anat] 1980, 387: 147–164